

Radical chiral Floquet phases in a periodically driven Kitaev model and beyond

Hoi Chun Po,^{1,2} Lukasz Fidkowski,^{3,4} Ashvin Vishwanath,^{1,2} and Andrew C. Potter⁵

¹*Department of Physics, University of California, Berkeley, CA 94720, USA*

²*Department of Physics, Harvard University, Cambridge MA 02138, USA*

³*Department of Physics and Astronomy, Stony Brook University, Stony Brook, NY 11794, USA*

⁴*Kavli Institute for Theoretical Physics, University of California, Santa Barbara, CA 93106, USA*

⁵*Department of Physics, University of Texas at Austin, Austin, TX 78712, USA*

Time periodic driving serves not only as a convenient way to engineer effective Hamiltonians, but also as a means to produce intrinsically dynamical phases that do not exist in the static limit. A recent example of the latter are 2D chiral Floquet (CF) phases exhibiting anomalous edge dynamics that pump discrete packets of quantum information along one direction. In non-fractionalized systems with only bosonic excitations, this pumping is quantified by a dynamical topological index that is a rational number – highlighting its difference from the integer valued invariant underlying equilibrium chiral phases (e.g. quantum Hall systems). Here, we explore CF phases in systems with emergent anyon excitations that have fractional statistics (Abelian topological order). Despite the absence of mobile non-Abelian particles in these systems, external driving can supply the energy to pump otherwise immobile non-Abelian defects (sometimes called twist defects or genons) around the boundary, thereby transporting an irrational fractional number of quantum bits along the edge during each drive period. This enables new CF phases with chiral indices that are square roots of rational numbers, inspiring the label: “radical CF phases”. We demonstrate an unexpected bulk-boundary correspondence, in which the radical CF edge is tied to bulk dynamics that exchange electric and magnetic anyon excitations during each period. We construct solvable, stroboscopically driven versions of Kitaev’s honeycomb spin model that realize these radical CF phases, and discuss their stability against heating in strongly disordered many-body localized settings or in the limit of rapid driving as an exponentially long-lived pre-thermal phenomena.

Time-periodic driving provides a powerful tool to shape the properties of quantum matter, from changing its topological phase[1–3], to enabling entirely new non-equilibrium dynamical phases. These dynamical phases are characterized by properties forbidden in the thermal equilibrium, such as spontaneous time-translation symmetry breaking[4–7] or dynamical topological order[8–14]. The latter opens the door to a new realm of quantum topological phenomena, which has only barely begun to be explored.

A striking example are chiral Floquet (CF) phases[15–17] – 2D dynamical topological phases with inert bulk dynamics, but whose edges act as chiral quantum channels that pump discrete quanta of quantum information along the edge in a chiral fashion each driving period. These are, in a sense, dynamical analogs, of integer quantum Hall phases familiar from thermal equilibrium settings, which can also occur in non-interacting fermion systems, have ordinary bulk properties, and chirally propagating edges that are protected even in the absence of any symmetry. However, CF phases are sharply distinct from integer quantum Hall systems. For example, their edge states exhibit a discrete pumping of quantum information rather than continuous flow of heat and charge. Moreover, CF phases are not captured by the usual equilibrium concepts like Chern numbers and Hall conductance[15], but are instead characterized by a new type of intrinsically dynamical topological invariant, the chiral unitary invariant ν . In interacting but non-fractionalized boson (spin) systems, ν takes the form $\log r$ where r is a positive rational fraction representing the ratio of states being pumped clockwise to counter-

clockwise around the edge[16]. For this reason, we dub these phases “rational” CF phases.

In equilibrium settings, strong interactions can effectively fracture the original microscopic particles into emergent excitations with fractional (anyonic) statistics, leading to new types of topological behavior like the fractional quantum Hall effect. Given the rough parallels between rational CF phases and the integer quantum Hall effect, it is natural to ask: Can strong interactions also produce new “fractional” CF phases? In this paper, we answer this question in the affirmative. We construct examples (including solvable lattice models) of systems whose edges chirally pump an irrational number of quantum states per driving period, which we dub radical chiral Floquet phases. Here we choose the nomenclature “radical” rather than “irrational” as these phases have chiral unitary index of the form $\nu = \log \sqrt{r}$ where r is a positive rational number. The existence of these radical CF phases relies crucially on the emergence of a particular type of Floquet-enriched topological order (FET)[18], with anyon excitations whose topological charges are dynamically transmuted during each driving period.

Our setup throughout will be a 2D lattice with a finite number of quantum degrees of freedom on each site, subjected to a time-periodic Hamiltonian $H(t) = H(t + T)$ with period T , and associated Floquet operator (time-evolution operator for one period):

$$U(T) = \mathcal{T} e^{-i \int_0^T H(t) dt}, \quad (1)$$

where \mathcal{T} denotes time-ordering. An important concern is whether driving will induce heating and destroy quan-

tum coherence. In generic systems, rapid driving can postpone heating for an exponentially long time, leading to a long-lived metastable “pre-thermal” regime[19] with quantum coherent non-equilibrium dynamics[20]. Even more strikingly, in isolated systems such as cold-atoms and trapped ions, heating can be avoided entirely by synthesizing sufficiently strong disorder drive the system into a many-body localized (MBL) regime[21], where it cannot absorb energy from the drive and remains quantum coherent, in principle, indefinitely[22]. We will focus on the latter MBL case, though our discussion also enables a construction of pre-thermal versions of these phases.

Review of rational Chiral Floquet phases – In the absence of fractionalized anyonic excitations, and in the MBL regime, the Floquet evolution operator decomposes into commuting bulk and edge pieces. The edge evolution acts within a finite strip at the system boundary, and describes an effectively one-dimensional evolution. Such locality-preserving 1D unitary time evolutions are exhaustively characterized by a rational fraction, r , characterizing the ratio of quantum states being pumped right versus left across any spatial cut at the edge[23]. In a pure 1D system there must be an exact balance of quantum state flow, $r = 1$, so that states cannot pile up or be depleted from the ends of the system (otherwise the quantum dynamics cannot respect both unitarity and locality). However, the boundary of a 2D system forms a closed loop and does not face this difficulty, and can realize any rational index, r [16]. We remark that it is convenient to convert the “number of quantum states” into an additive measure of chiral quantum “entropy” flow, by taking the logarithm of r , which defines the chiral unitary index: $\nu = \log r$. A non-zero value of ν necessarily arises from having a topologically nontrivial bulk dynamics. Further, ν cannot be altered by any local edge perturbation, but only via a bulk dynamical phase transition.

Solvable models with such CF behavior were originally constructed for free fermion systems[8, 15, 24] which realize a subset of chiral unitary indices: $\nu = n \log 2$ for integer n . CF phases were subsequently shown to be stable to interactions[16, 17], and generalized to generic interacting bosonic systems that can realize $\nu = \log r$ for any rational fraction r [16]. These models share a common structure in which bulk degrees of freedom traverse circles in short closed loops and edge particles or spins are pumped chirally around the sample boundary[25].

Spin model – We begin by constructing a solvable lattice model, based on a stroboscopically driven version of Kitaev’s honeycomb spin model[26]. This model will enable controlled insight into the general structure of radical CF phases. Starting from an ordinary lattice of spin-1/2 degrees of freedom with two states per site, our strategy will be to dynamically induce \mathbb{Z}_2 topological order thereby liberating emergent fermion excitations. The edge of the model will then act as a chiral edge pump for non-Abelian (Majorana) defects of this topological

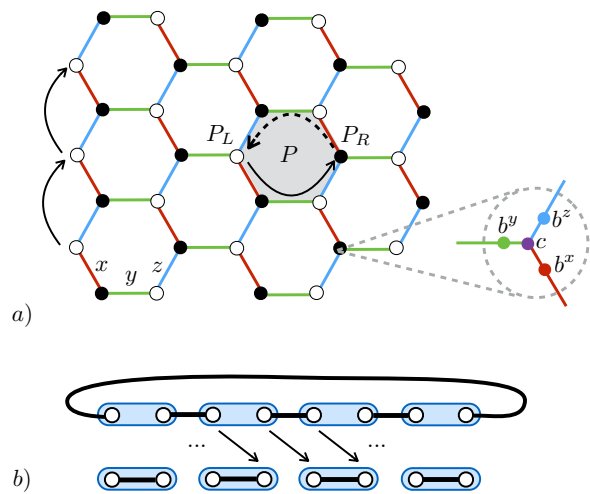


FIG. 1. **Spin-1/2 Honeycomb model** – (a) Depiction of solvable lattice for a radical chiral Floquet phase and Majorana fermion description. (b) The topological and trivial phases of a chain of complex fermions (blue boxes indicate fermion sites) can be viewed as two topologically distinct ways to pair (black lines) adjacent Majorana fermions (open circles). Under an open boundary condition these two phases are distinguished by the presence or absence of unpaired edge Majorana fermions, but with periodic boundary condition they are related by a chiral translation of the Majorana fermions (arrows).

order that each carry an irrational amount, $\log \sqrt{2}$, of quantum information. We will first construct an idealized fixed-point drive with uniform couplings. Weakly perturbing this uniform model produces a long-lived pre-thermal phase upon weak perturbations. Alternatively, we may add strong disorder to convert it into a stable MBL phase (see Appendix B).

Inspired by Kitaev’s construction[26], we take spin-1/2 degrees of freedom, \vec{S}_r , sitting on sites r of a honeycomb. The three distinct types of bonds of the honeycomb are labeled by x , y , and z respectively, and we embed the fermionic degrees of freedom as shown in Fig. 1a. The idealized drive consists of a three-step stroboscopic time evolution obtained by cycling through the Hamiltonians $H(t) = \frac{3}{T} h^{[j(t)]}$ applied in the sequence: $j = x, y, z$, each for time $T/3$, so that the Floquet evolution operator is:

$$U(T) = e^{-ih^{[z]}} e^{-ih^{[y]}} e^{-ih^{[x]}}, \quad h^{[j]} = \frac{\pi J}{4} \sum_{\langle rr' \rangle \in j} S_r^j S_{r'}^j \quad (2)$$

In the limit of weak driving ($J \ll 1$), $U(T)$ realizes a conventional static phase with \mathbb{Z}_2 topological order featuring an emergent gapless Majorana fermion[26]. However, we will instead consider the strong driving limit: $J = 1$.

To analyze this model, Eq. (2), following[26], we rewrite each spin-1/2 in terms of four Majorana fermion

operators, $\{c_r, b_r^{x,y,z}\}$, as:

$$S_r^i = i c_r b_r^i, \quad (3)$$

which introduces a local \mathbb{Z}_2 gauge redundancy generated by $(c_r, \vec{b}_r) \rightarrow (-1)(c_r, \vec{b}_r)$, and must be subjected to the gauge-neutral sector via the on-site constraints $(-i S_r^x S_r^y S_r^z) = (c_r b_r^x b_r^y b_r^z) = 1$ to faithfully describe the spin-1/2 Hilbert space. We can draw the Majorana fermion degrees of freedom such that c_r resides on the honeycomb sites, and b_r^i reside on the links of type i (see Fig. 1a). It is convenient to pair the \vec{b}_r Majorana operators into \mathbb{Z}_2 gauge link variables $\sigma_{r,r'} = i b_r^j b_{r'}^j$, where $j \in \{x, y, z\}$ according to the type of link $\langle r, r' \rangle$, and where we take an arbitrary fixed orientation of $r \rightarrow r'$ on each type of bond.

Each factor of $e^{-ih[j]}$ drives the hopping of Majorana fermions: $e^{ih[j]} c_r e^{-ih[j]} = c_{r+\hat{e}_j} \sigma_{r,r+\hat{e}_j}$ where \hat{e}_j is the oriented unit vector along the type- j bonds, and leaves the gauge links $\sigma_{r,r'}$ unaffected.

The gauge link variables $\sigma_{r,r'}$ are invariant under the Floquet evolution, which we can express as a conservation of gauge flux:

$$\mathcal{F}_P = \prod_{\langle rr' \rangle \in \partial P} \sigma_{r,r'}, \quad (4)$$

through each hexagonal plaquette, P .

In the bulk, the c Majorana fermions are driven in small counter-clockwise loops, encircling their respective plaquettes after two driving periods (Fig. 1a) and accumulates a \mathbb{Z}_2 -valued Aharonov-Bohm phase \mathcal{F}_P along the way. While seemingly innocuous on first glance, this phase will play a crucial role in enabling the radical CF edge physics.

Edge chiral index – In contrast to their bulk counterparts, the c Majoranas at the edge are driven in a large clockwise loop around the entire system boundary, such that an odd number of Majorana fermions cross any cut through the edge during each driving cycle. Since each Majorana degree of freedom has “half” the number of degrees of freedom as a fermion, it corresponds to $\sqrt{2}$ quantum states, and hence we expect a radical chiral unitary index $\nu = \log \sqrt{2}$.

We can confirm this expectation by the following trick: instead of computing the index ν for $U(T)$ directly, we can consider the time evolution for two periods, $U(2T)$, whose edge turns out to be governed by a rational chiral unitary index $\nu_{2T} = 2\nu$. The index, ν_{2T} can be computed by the algebraic method of Refs. [16, 23]. The quantum information pumped across a cut in the edge during each period is quantified by taking a basis of observables on one side of a cut in the edge, evolving them forward in time, and evaluating its overlap with observables on the other side of the cut. The chiral topological index is then the logarithm of the ratio of the quantum information being pumped right to that being pumped left per period. A relatively straightforward computation (Appendix A),

using strings of spin operators $S_i^{x,y,z}$ as a basis for operators, shows that $\nu_{2T} = \log 2$, i.e.:

$$\nu = \frac{1}{2} \nu_{2T} = \log \sqrt{2}, \quad (5)$$

confirming that this model indeed realizes a radical CF phase.

Bulk properties – To characterize the bulk dynamics, we can pair the bulk Majoranas on the left and right sides of each hexagonal plaquette into complex fermion orbitals, $\psi_P = \frac{1}{2}(c_{P_L} + i W_{\hat{P}} c_{P_R})$, where $W_{\hat{P}} \equiv \sigma_{\swarrow} \sigma_{\leftarrow} \sigma_{\nwarrow}$ is a gauge string connecting the sites $P_{R/L}$ via a counter-clockwise loop over the top of plaquette P (dashed curved arrow in Fig. 1a). The plaquette fermion orbitals can be either occupied or empty, corresponding respectively to local fermion parity: $\mathcal{P}_P = (-1)^{\psi_P^\dagger \psi_P} = \pm 1$.

After one Floquet period, $\mathcal{P}_P \rightarrow \mathcal{F}_P \mathcal{P}_P$ due to the Aharonov-Bohm phase mentioned above. In other words, the plaquette Fermion parity is conserved on gauge-flux-free plaquettes ($\mathcal{F}_P = +1$), and is flipped on plaquettes with a flux ($\mathcal{F}_P = -1$).

To physically interpret this result, first note that the fact that bulk gauge fluxes have no quantum fluctuations, which indicates the bulk Floquet operator has a dynamical \mathbb{Z}_2 topological order, with three topologically distinct types of anyon excitations: a fermion ψ ($\mathcal{P}_P = -1$, $\mathcal{F}_P = +1$), a bosonic flux m ($\mathcal{P}_P = -1$, $\mathcal{F}_P = +1$), and their bosonic bound state: $e = m \times \psi$, each having mutual statistics (-1) with the others. The Floquet evolution conserves the number of ψ particles on each plaquette, $n_{\psi,P}$, and the total number gauge fluxes (either e or m particles): $n_{F,P} = (n_{e,P} + n_{m,P})$. During each driving period, e anyons are transmuted into m anyons and vice versa, a phenomena dubbed Floquet enriched topological order (FET)[18].

Since the bulk Floquet evolution does not produce kinetic motion of any of the bulk anyon particles, it appears naturally amenable to MBL. Indeed, in Appendix B, we argue that a disordered version of this Hamiltonian produces a stable MBL phase, albeit one that exhibits time-translation symmetry breaking[6] due to the continual period- $2T$ flip-flopping of e and m particles[18]. Having solved the bulk dynamics of this model, we turn to its edge state properties, and examine the correspondence between bulk-FET order and edge radical CF order.

Bulk-boundary correspondence – We saw that the radical chiral Floquet nature of the edge was accompanied by FET order in the bulk. Next, we argue that these two phenomena are inextricably linked.

To build some intuition, we first recall that the $e \leftrightarrow m$ exchanging FET order can be viewed as arising from a dynamical pumping of loops of 1D topological chains of the ψ -fermions onto the systems boundary during each Floquet period[18], which toggles the 1D chain of fermions at the edge between the topological and trivial phases. Since the fermion parity of the 1D topological fermion chain is flipped by insertion of a π -flux[27], this

pumping adds a fermion to bulk gauge fluxes, and interchanges e and m particles. By formally decomposing each complex fermion degree of freedom at the edge into a pair of Majorana fermions, one can see that the chiral Majorana translation at the edge of the radical CF phase toggles the 1D topological invariant of the edge (Fig. 1b). In this picture, the chiral translation modifies the pairing patterns of the Majorana fermions, which amounts to changing the topological phase of this 1D complex fermion chain[27]. More generally, this picture immediately shows that any odd number of Majorana translations at the edge will produce the accompanying FET order, whereas even number of translations will not. This suggests that the radical chiral edge index always appears with bulk FET order.

To further support this conjecture, we can work in the limit of well-localized gauge fluxes, so that the above problem reduces to that of non-interacting Majorana fermions in a static gauge-flux background. In this non-interacting limit, we can directly show that the radical part of the chiral edge invariant is related to the bulk FET order as (see Appendix C):

$$e^{2\pi i \nu_{\text{edge}} / \log 2} = \mathcal{I}_{\text{FET}} \quad (6)$$

where \mathcal{I}_{FET} is the \mathbb{Z}_2 -valued bulk FET invariant defined as -1 in the FET phase and $+1$ in the trivial phase. We note that, this relation can be rigorously established beyond the free fermion limit by generalizing the rigorous machinery for chiral unitary invariants[16, 23] to incorporate fermionic super-algebras[28].

The concurrent appearance of FET order also explains how this model can exhibit irrational values of the chiral edge index. So long as we may factorize the Floquet evolution into commuting bulk and edge pieces, the chiral unitary index will be rational [16, 23].[29] However, this decomposition fails in a radical CF phase precisely due to the presence of the FET order. Specifically, in the sector with an odd number \mathbb{Z}_2 gauge fluxes in the bulk, the Floquet evolution transfers an odd number of fermions from bulk to boundary, such that the bulk and boundary factors in $U(T)$ would be anti-commuting fermionic operators. This failure to factorize into commuting bulk and edge pieces exposes a loophole in the rational classification[16], and allows for radical chiral edge invariants.

Parafermionic generalizations – In the driven \mathbb{Z}_2 -topologically ordered example above, we found that, despite that the system has only integer-dimension Abelian anyon excitations, it exhibited a chiral edge pumping of effectively non-Abelian objects with irrational quantum dimension $\sqrt{2}$. The resolution to this apparent contradiction is this: since we are explicitly driving the system in a time-dependent fashion, energy is not conserved, and we may pump certain confined defects of the Abelian topological order around the edge, without these defects appearing as deconfined bulk quasi-particles. Namely, the Majorana fermions in the above example can be

viewed as the ends of topological chains of the emergent fermionic quasi-particles, (or equivalently as “twist” defects that exchange e and m particles[30, 31]), which have irrational quantum dimension $d = \sqrt{2}$.

We can readily generalize the spin-1/2 construction to obtain other radical CF phases characterized by chiral edge pumping of defects of more general topological orders. For simplicity, and to retain the possibility of MBL[32], we will restrict ourselves to Floquet drives with Abelian bulk topological order and vanishing Hall conductance[33]. A simple extension that captures the general structure of such Abelian radical CF phases is to consider a driven \mathbb{Z}_N topological order for general integer N , whose excitations consist of bosonic \mathbb{Z}_N gauge fluxes, m , (satisfying $m^N = 1$), and anyonic gauge charge, ψ , with fractional statistics $\theta_\psi = e^{2\pi i/N}$, and various bound states such as $e = m \times \psi^{-1}$. Following the footsteps of the \mathbb{Z}_2 example above, we can fractionalize the ψ particles into pairs of parafermionic defects with quantum dimension \sqrt{N} (which can be viewed as edge states of 1D topological chains of ψ particles, generalizing the Majorana case for $N = 2$, or as twist defects that interchange e and m particles). One can consider a regular lattice of these parafermionic defects, subjected to a Floquet drive that pumps them around closed loops in the bulk and around large open chiral orbits at the boundary, resulting in a radical chiral edge index $\nu = \log \sqrt{N}$. An explicit solvable lattice model with such properties can be readily obtained by a straightforward generalization of the driven honeycomb spin model with spins- $\frac{N-1}{2}$ (see Appendix D).

As for the \mathbb{Z}_2 case, the action of translating edge parafermions by one (or more generally an odd number of) sites interchanges the trivial and topological parafermion phases on the 1D boundary (see Fig. 1b), and hence produces bulk FET order characterized by a dynamical interchanging of $e \leftrightarrow m$ particles. The bulk FET nature again causes a failure of the Floquet evolution to factorize into commuting bulk and edge parts, since in the sector with j gauge fluxes in the bulk, j anyonic ψ particles are transferred from bulk to edge. The anyonic character of the bulk action of $U(T)$ allows the system to elude the restriction to rational edge indices[16, 23], since the evolution does not factorize into commuting bulk and edge pieces, but rather into a sum over bulk-gauge flux sectors, with non-commuting bulk and edge pieces:

$$U(T) = V \left(\bigoplus_{j=0}^N \Psi_{\text{bulk}}^{(j)} \Psi_{\text{edge}}^{(j)} \right) V^\dagger \quad (7)$$

where $\Psi_{\text{edge/bulk}}^{(j)}$ are non-commuting *anyonic* operators with topological spin $e^{\pm 2\pi j/N}$ respectively, j denotes the bulk gauge flux, and $V = e^{-i\mathcal{H}}$ is a local unitary transformation generated by local Hamiltonian \mathcal{H} (i.e. a local basis transformation). Again, we notice that time evolution by two periods returns all bulk anyons to their original state, so that $U(2T)$ can be written as a product

of bosonic bulk and edge terms, which are hence governed by a rational chiral index[16].

Discussion – We have so far considered a system with bosonic (spin) degrees of freedom, where the emergence of a radical chiral edge requires Majorana fermion defects arising from emergent fermion degrees of freedom. In fermionic systems, such Majorana defects are already present, and a radical CF phase with $\nu = \log \sqrt{2}$ can be obtained without any accompanying bulk topological order[16, 28]. An important caveat is that, this phase requires the breaking of fermion-number conservation through pair condensation of the fermions. This pair condensation prevents MBL[32], but may be realized as a prethermal phenomena[20].

While we have focused on the case of Abelian bulk topological order, with an eye towards leveraging MBL to stabilize the system against bulk heating, one could also consider metastable chiral Floquet phases arising in systems with non-Abelian bulk topological order in a prethermal regime[19, 20]. A direct anyonic generalization of the bosonic SWAP model of Ref. [16] is obtained by taking a square lattice of non-Abelian particles, and replacing the SWAP terms by pair-wise braidings, resulting in a chiral translation of non-Abelian anyons at the system boundary. Intuitively, such construction gives rise to a phase with chiral unitary index $\nu = \log d$, where d is the quantum dimension of the anyon in question. However, we leave a more systematic study of such non-Abelian generalizations of CF phases for future work.

Acknowledgements – LF is supported by NSF DMR-1519579 and by Sloan FG-2015- 65244. AV acknowledges support from a Simons Investigator Award and AFOSR MURI grant FA9550-14-1-0035. This research was supported in part by the Kavli Institute of Theoretical Physics and the National Science Foundation under Grant No. NSF PHY11-25915.

Appendix A: Computation of the chiral index for the spin-1/2 honeycomb model

In this appendix, we solve $U(2T)$ exactly by recognizing a connection of the model to the stabilizer formalism in quantum computing. We will then establish that the chiral unitary index ν of $U(2T)$, which is well-defined despite the MBL intrinsic topological order in the bulk, is $\nu[U(2T)] = \log 2$.

1. Clifford circuits

We begin by reviewing the pertinent preliminaries of the stabilizer formalism. Consider a quantum system of n qubits (spin-1/2's) labeled by $r = 1, \dots, n$. For each qubit we have the Pauli operators X_r, Y_r and Z_r , and we consider the *Pauli group of n qubits* $P_n \equiv \{\alpha \sigma_1 \otimes \sigma_2 \otimes \dots \otimes \sigma_n : \alpha \in \{1, i, -1, -i\}, \sigma_r \in \{1, X_r, Y_r, Z_r\}\}$. We say a unitary operator U is a *Clifford operation* if

$\forall \sigma \in P_n, U\sigma U^\dagger \in P_n$, i.e. under conjugation by U ‘Pauli products’ remain as ‘Pauli products’. Up to an irrelevant overall $U(1)$ phase, a Clifford operation is uniquely determined by its action on the Pauli group.

To connect with the problem at hand, first we note that all the two-qubit gates involved in $U(T)$ are Clifford operations. For example:

$$e^{-i\pi X_1 X_2/4} Z_2 e^{i\pi X_1 X_2/4} = \frac{i}{2} X_1 [Z_2, X_2] = -X_1 Y_2, \quad (\text{A1})$$

and similarly for all other combinations of gates and Pauli operators. This implies $U(2T)$ is a Clifford circuit, and by the previous discussion it is specified by its action on the Pauli operators. The action of $U(2T)$ on single-site operators $\sigma_r \in \{X_r, Y_r, Z_r\}$ are represented graphically in Fig. 2. Together with the symmetries of the problem, this completely specifies $U(2T)$ as a Clifford circuit.

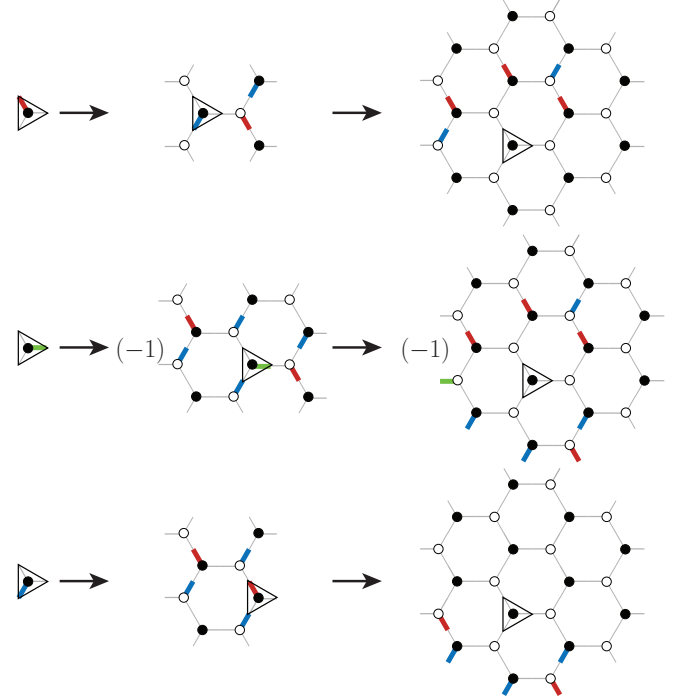


FIG. 2. **Evolution of Pauli operators.** The three Pauli operators associated to each site (filled or open circle) are represented graphically as a colored, thickened line along the corresponding bond. The same color scheme as in Fig. 1 is used, where red, green and blue respectively represent X_r, Y_r and Z_r . The triangles indicate the positions of the original sites, and the arrows indicate time evolution by $U(T)$.

2. Factorization of $U(2T)$ into bulk and edge pieces

As discussed in the main text, $U(2T)$ admits a complete set of local integrals of motion $\{\mathcal{F}_P, \mathcal{P}_P\}$, where P runs over all plaquettes in the system. This suggests

$U(2T)$ factorizes into a mutually commuting product of local unitary operations. Here, we demonstrate this by writing down a closed-form expression of $U(2T)$, which then allows us to compute its chiral edge invariant via the GNVW formalism[16, 23].

Since $U(2T)$ conserves $\{\mathcal{F}_P, \mathcal{P}_P\}$, we can construct it from the projection operator onto the plaquette flux: $\mathcal{V}_P \equiv (1 - \mathcal{F}_P)/2$. Recall that $U(2T)$ applies a phase \mathcal{F}_P to the Majorana operators c_r . Together with the translation invariance of Eq. (2), this property suggests:

$$U(2T) \stackrel{?}{=} G_\phi \equiv \prod_P ((1 - \mathcal{V}_P) + e^{i\phi} \mathcal{V}_P \mathcal{P}_P), \quad (\text{A2})$$

where $e^{i\phi}$ is a *physical* $U(1)$ phase that is to-be-determined, and the equality holds up to an unimportant overall phase.

To verify Eq. (A2), we compute the evolution of a spin operator σ_r under conjugation by G_ϕ . As \mathcal{F}_P and \mathcal{P}_P are also product of Pauli operators, we have $\mathcal{F}_P \sigma_r = \zeta(\mathcal{F}_P, \sigma_r) \sigma_r \mathcal{F}_P$ and $\mathcal{P}_P \sigma_r = \zeta(\mathcal{P}_P, \sigma_r) \sigma_r \mathcal{P}_P$, where $\zeta = \pm 1$. Therefore, given σ_r and a particular plaquette P_0 there are only four possible results, as tabulated in Table I.

TABLE I. Transformation of a spin operator σ_r under a single-plaquette factor, labeled by P_0 , in $G_\phi = \prod_P G_{\phi, P}$.

$\zeta(\mathcal{F}_{P_0}, \sigma_r)$	$\zeta(\mathcal{P}_{P_0}, \sigma_r)$	$G_{\phi, P_0} \sigma_r G_{\phi, P_0}^\dagger$
+	+	σ_r
+	-	$\mathcal{F}_{P_0} \sigma_r$
-	+	$\exp(-i\phi \mathcal{F}_{P_0}) \mathcal{P}_{P_0} \sigma_r$
-	-	$-\exp(-i\phi \mathcal{F}_{P_0}) \mathcal{F}_{P_0} \mathcal{P}_{P_0} \sigma_r$

Computing the evolution of X_r , one sees that G_ϕ could be identified with $U(2T)$ only if $\phi = 0$ or π , which we denote respectively by G_+ and G_- . Furthermore, one can verify that both G_\pm reproduce the correct evolution of all Pauli operators in Fig. 2, and from the discussion in the previous subsection the guess in Eq. (A2) is verified – except that we have found *two* solutions even when the Clifford circuit is uniquely determined up to the global phase. In addition, one can check that the π -rotation about the center of a hexagon, a symmetry of the model, exchanges $G_+ \leftrightarrow G_-$, and so apparently neither of them can be a solution. These paradoxes are resolved by noticing the following:

$$G_+ G_-^\dagger = \prod_P ((1 - \mathcal{V}_P) - \mathcal{V}_P) = \prod_P \mathcal{F}_P = 1, \quad (\text{A3})$$

where the last equality holds for periodic boundary condition. This establishes $G_+ = G_-$, and hence we conclude $U(2T) = G_\pm$. Note that G_\pm is a product of mutually commuting local unitaries, and therefore $U(2T)$ manifestly factorizes into bulk commuting and edge pieces, and that its edge is characterized by a rational chiral unitary invariant.

From the discussion in Ref. [16], when the system is put on a geometry with OBC one can write $U(2T) = Y_{\text{edge}} U_{\text{bulk}}$ with exponential accuracy, where Y_{edge} is a quasi-1D unitary acting nontrivially only near the edges. Note that this procedure is unaffected by the fact that $U(2T)$ features intrinsic topological order in the bulk, and so the chiral unitary index of Y_{edge} is well-defined and remains as a diagnostic of the chiral nature of the model. In addition, the computed index is stable against small perturbation that maintains the MBL nature of the bulk – and in the present case such robustness can be achieved by appending to the driving protocol a fourth disordering step. (See also Appendix B for a elaborated discussion on disordering.)

3. Chiral unitary index of $U(2T)$

The chiral unitary index ν of $U(2T)$ can be computed following the discussion in Ref. [16], where the edge unitary Y_{edge} is exposed by ‘undoing’ the bulk dynamics using the truncation of the periodic-boundary-condition evolution to the disk geometry. (For notational clarity we drop the subscript ‘edge’ on Y henceforth.) As a minor technical remark, we note that the truncation of G_+ and G_- do not agree, as they differ by the global flux operator on the disk. However, this mismatch, being a Pauli product along the boundary, is manifestly a locally-generated unitary, and therefore ν remains well-defined. In the following, Y is defined using G_+ .

To efficiently evaluate $\nu(Y)$, we first tailor the original index formula in Refs. [16 and 23] into a form optimized for a Clifford circuit. Recall the overlap η of two local operator algebras \mathcal{A} and \mathcal{B} is defined as

$$\eta(\mathcal{A}, \mathcal{B}) \equiv \frac{\sqrt{p_a p_b}}{p_\Lambda} \sqrt{\sum_{\mu=1}^{p_a} \sum_{\nu=1}^{p_b} \left| \text{Tr}_\Lambda \left(e_\mu^{a\dagger} e_\nu^b \right) \right|^2}, \quad (\text{A4})$$

where μ (ν) indexes a complete set of basis for \mathcal{A} (\mathcal{B}). To take advantage of the Clifford structure, we choose a standard basis for an interval with l sites labeled by the multi-index $\mu \equiv (\mu_1, \dots, \mu_l)$, defined through $\sigma_\mu^L \equiv \sigma_{\mu_1} \otimes \sigma_{\mu_2} \otimes \dots \otimes \sigma_{\mu_l}$, where $\mu_i \in \{0, 1, 2, 3\}$ labels the Pauli matrices in the standard convention.

The chiral unitary index is then defined as

$$\nu(Y) \equiv \log \frac{\eta(Y(\mathcal{A}_L), \mathcal{A}_R)}{\eta(\mathcal{A}_L, Y(\mathcal{A}_R))}, \quad (\text{A5})$$

where \mathcal{A}_L and \mathcal{A}_R respectively denote the operator algebras (with a sufficiently large size) on the left and right of a specified spatial cut, and $Y(\mathcal{A}) \equiv \{Y e Y^\dagger : e \in \mathcal{A}\}$ is the transformed algebra.

As σ_{μ_i} is traceless for $\mu_i = 1, 2, 3$, only terms with $\sigma^a = \sigma^b$ can contribute in the trace in Eq. (A4). In

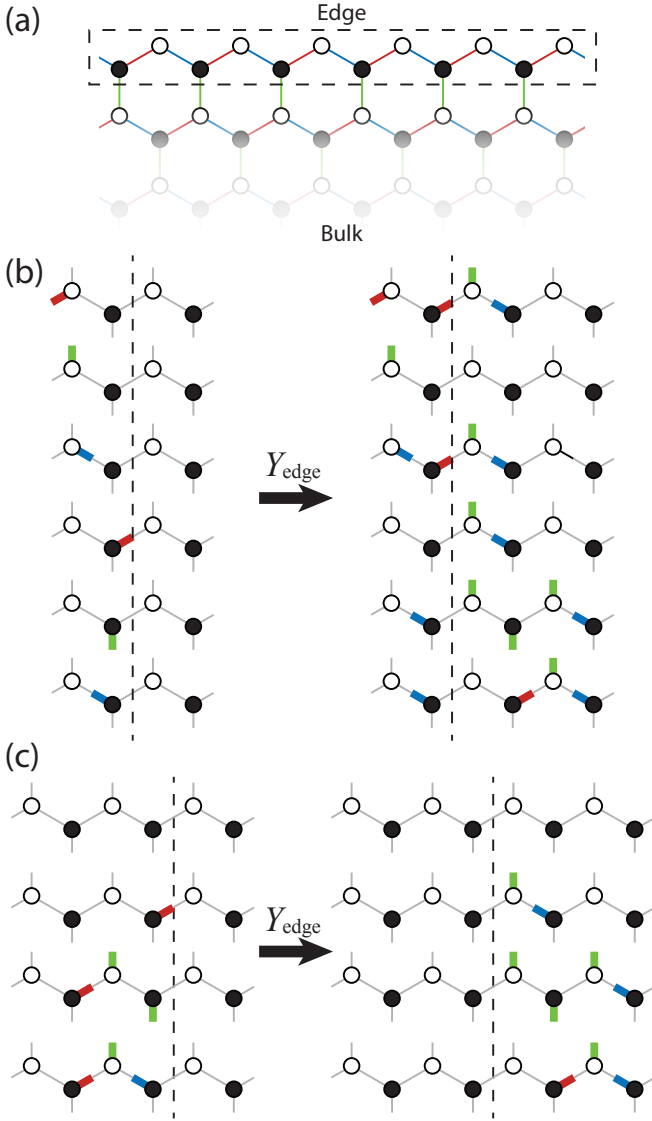


FIG. 3. **Chiral unitary index ν of $U(2T)$.** (a) The index is computed for the indicated edge, where the boxed region (of depth being one lattice constant) corresponds to where the edge unitary Y_{edge} acts nontrivially. Note that we have rotated the lattice by 90° relative to Fig. 1. (b) As the chosen edge retains lattice translation invariance along the parallel direction, Y_{edge} (also a Clifford circuit) is fully specified by computing the evolution of the six Pauli operators associated with the two inequivalent sites in a unit cell. The Pauli operators are represented in the same way as Fig. 2, and we do not keep track of the global phase as it does not enter the index computation. The vertical dashed line indicates a fixed spatial cut. (c) Using the evolution in (b), one sees that exactly four Pauli operators are ‘transported’ from the left to the right of the cut, and only one (the identity) from right to left. This gives $\nu[U(2T)] = \log \sqrt{4} = \log 2$.

addition, as Y is a Clifford circuit, generally one finds

$$Y \left(\bigotimes_{i \in L} \sigma_{\mu_i} \right) Y^\dagger = \pm \left(\bigotimes_{i \in L} \sigma_{\mu'_i} \right) \otimes \left(\bigotimes_{j \in R} \sigma_{\nu_j} \right), \quad (\text{A6})$$

and we say $\bigotimes_{i \in L} \sigma_{\mu_i}$ is ‘transported across the cut’ if $\mu'_i = 0 \forall i$, i.e. $(Y \sigma_\mu^L Y^\dagger)|_L = 1$ (this includes, in particular, the identity). These are the only operators that can contribute in $\eta(Y \mathcal{A}_L Y^\dagger, \mathcal{A}_R)$, and each such term contribute with the same weight as the identity. Therefore the index formula for a Clifford circuit is simply a counting formula:

$$\nu(Y) \stackrel{\text{Clifford}}{=} \log \sqrt{\frac{|\{\sigma_\mu^L : (Y \sigma_\mu^L Y^\dagger)|_L = 1\}|}{|\{\sigma_\nu^R : (Y \sigma_\nu^R Y^\dagger)|_R = 1\}|}}. \quad (\text{A7})$$

The computation is detailed in Fig. 3, which shows that $\nu[U(2T)] = \log 2$ – the minimal possible value in a spin-1/2 system. As discussed in the main text, this implies $\nu[U(T)] = \frac{1}{2} \nu[U(2T)] = \log \sqrt{2}$, which falls outside of the original GNVW classification. Such a radical index is allowed because, unlike $U(2T)$, $U(T)$ cannot be factorized into commuting bulk and edge pieces due to the bulk FET order.

Appendix B: Radical CF phase at strong disorder

In the main text we have examined a zero-correlation length ‘fixed point’ honeycomb spin-1/2 model for a radical CF phase with no disorder. We can attempt to extend this into a stable MBL phase by adding a fourth driving step with strongly random disorder coupling to the local conserved quantities of the clean driving steps in Eq. (2), so that $U(T)$ becomes $\tilde{U}(T) = e^{-i h_{\text{dis}}} e^{-i h^{[z]}} e^{-i h^{[y]}} e^{-i h^{[x]}}$, with:

$$h_{\text{dis}} = - \sum_P \sum_{a=e,m,\psi} \mu_{a,P} n_{a,P} \quad (\text{B1})$$

Here, $\mu_{a,P}$ is a random potential for an anyon excitation of type a on plaquette P .

The local plaquette fermion number, $n_{\psi,P}$, and the total gauge flux $n_{e,P} + n_{m,P}$ are conserved by the clean part of the drive, $U(T)$. However, the difference between the number of e and m particles is flipped by $U(T)$ due to the FET order. Despite that h_{dis} does not fully commute with $U(T)$, we can still readily write down exact eigenstates of the disordered drive, $\tilde{U}(T)$.

Denote a fixed configuration of anyon excitations as: \mathcal{C} , and its energy, and the related configuration obtained by interchanging all e and m particles in \mathcal{C} as \mathcal{C}' . The energy difference between \mathcal{C} and \mathcal{C}' with respect to h_{dis} is: $\delta E = \sum_P (\mu_{e,P} - \mu_{m,P}) n_{e,P}(\mathcal{C})$. Denoting the the number of anyons of type a on plaquette P in configuration \mathcal{C} as $n_{a,P}(\mathcal{C})$, we can write down the energy of configurations

\mathcal{C} and \mathcal{C}' with respect to the disorder Hamiltonian h_{dis} :

$$\begin{aligned} E_{\mathcal{C}} &= - \sum_{a,P} \mu_{a,P} n_{a,P}(\mathcal{C}) \equiv E_0(\mathcal{C}) + \Delta E(\mathcal{C}) \\ E_{\mathcal{C}'} &= - \sum_{a,P} \mu_{a,P} n_{a,P}(\mathcal{C}') \equiv E_0(\mathcal{C}') - \Delta E(\mathcal{C}') \\ E_0(\mathcal{C}) &= - \sum_P \mu_{\psi,P} n_{\psi,P}(\mathcal{C}) + \frac{\mu_{e,P} + \mu_{m,P}}{2} n_{e,P}(\mathcal{C}) \\ \Delta E &= - \sum_P \frac{\mu_{e,P} - \mu_{m,P}}{2} n_{e,P}(\mathcal{C}) \end{aligned} \quad (\text{B2})$$

From this, we can readily identify a pair of Floquet eigenstates of $\tilde{U}(T)$:

$$|\psi_{\pm}\rangle = \frac{1}{\sqrt{2}} \left(e^{i\Delta E/2} |\mathcal{C}\rangle \pm e^{-i\Delta E/2} |\mathcal{C}'\rangle \right) \quad (\text{B3})$$

which have quasi-energies $\epsilon_+ = E_0(\mathcal{C})$, $\epsilon_- = E_0 + \pi$, which differ exactly by π . This form of eigenstates are exactly those of a Floquet time-crystal with spontaneous period doubling [6], as a system initially prepared in state $|\mathcal{C}\rangle$ will oscillate between $|\mathcal{C}\rangle$ and $|\mathcal{C}'\rangle$ from one period to the next.

However, this is not the end of the story, because there are actually an extensive number of other pairs of eigenstates that also have quasi-energies $(E_0, E_0 + \pi)$, which can be obtained simply by flipping any number of e particles in \mathcal{C} with m -particles, resulting in an overall degeneracy:

$$D(\mathcal{C}) = 2^{\sum_P (n_{e,P}(\mathcal{C}) + n_{m,P}(\mathcal{C}) - 1)} \quad (\text{B4})$$

of states with quasi energy E_0 and $E_0 + \pi$ respectively, as if the e and m particles have been effectively promoted to quantum dimension 2 objects[18].

This degeneracy will be resolved by quantum fluctuations upon moving away from the zero-correlation length limit, by even an infinitesimal amount. However, due to the FET structure, the degenerate states cannot be split in such a way that preserves both their localized properties and time-translation symmetry[18, 32].

At strong disorder, a natural outcome is for quantum fluctuations to spontaneously select time-crystalline MBL states of the form shown in Eq. (B3). To proceed, let us consider the evolution for two periods, $U(2T)$ which can be written in the absence of an edge, as evolution under some effective topologically ordered Hamiltonian H_{eff} , with a symmetry between e and m particles, which derives from the dynamical permutation of e and m particles in $U(T)$ [18]. Let us consider moving away from the zero-correlation length limit with a generic but weak T -periodic perturbation, which corresponds to an $e \leftrightarrow m$ symmetry preserving perturbation to $H_{\text{eff}} \rightarrow H_{\text{eff}} + V$. Starting from a localized anyon configuration \mathcal{C} , we can restrict our attention to the degenerate space of anyon configurations with the same quasi-energy (modulo π) as \mathcal{C} , which we can model as a fermionic Hilbert space where each e/m particles is a fermion site that can either

be occupied or empty. The perturbation V induces quantum fluctuations that mix these degenerate states, which can be viewed as virtual anyon particle-hole pairs being created out of the “vacuum” and either annihilating.

To obtain a controlled description, we will assume that there is a low density of e/m particles in \mathcal{C} , typically separated by distance r , which is much greater than the strength of quantum fluctuations, Γ_0 compared to the RMS variations of μ_{ψ} , which defines a localization length scale: $\xi \approx 1/\log(\Delta\mu_{\text{psi}}/\Gamma_0)$.

There are two distinct types of these virtual processes that we will be interested in: First, virtually excited fermions land on an e or m particle toggling it to an m or e particle (such processes must occur in pairs to stay within the degenerate manifold of states associated with \mathcal{C}). With this process alone, we can model the system as a free fermion system, with a lattice of fermion sites corresponding to either e or m particles, which we will label by sites i , governed by the free fermion Hamiltonian $H_{\psi} \approx \sum_{ij} \Gamma_{ij} \psi_i \psi_j + \text{h.c.}$, where $\Gamma_{ij} \approx \Gamma_0 e^{-r_{ij}/\xi}$ are generically exponentially decaying in the distance between i and j , and ψ_i destroys a fermion on site i .

The second type of virtual processes of interest are those in which a pair of virtually excited e particles (or equivalent pair of virtual m particles) encircle a pair of fermion “sites”, which gives a different topological phase depending on whether or not both of the sites have the same occupation number. This corresponds to an interaction term between fermions $H_{\text{int}} \approx \sum_{ij} V_{ij} \left(\psi_i^{\dagger} \psi_i - \frac{1}{2} \right) \left(\psi_j^{\dagger} \psi_j - \frac{1}{2} \right) + \dots$, with $V_{ij} \approx \Gamma_0 e^{-2r_{ij}/\xi}$, and where the $+\dots$ indicates the contributions from virtual fluctuations that encircle higher numbers of fermion sites, which are suppressed by exponential distance factors compared to the leading term.

The problem of solving for the excited eigenstates of $H_{\psi} + H_{\text{int}}$ is complicated, but has been studied extensively in analogous 1D models [34], and we may draw lessons from this previous work. Namely, in 1D it was shown via a real-space renormalization group (RG) treatment, that, at strong disorder, the interaction terms were preserved under the RG flow, whereas the hopping terms flowed to zero. In the interaction dominated regime, the system naturally breaks the particle-hole symmetry, and forms a particle-hole asymmetric, fully localized state. An essentially identical strong disorder RG-based argument in 2D strongly suggests that the system will flow to the interaction dominated regime, even though the pair-tunneling amplitudes Γ_{ij} are typically much larger than the interaction strengths V_{ij} to begin with.

In the present context, the spontaneous particle-hole symmetry broken state corresponds to an MBL phase in which the dynamically $e \leftrightarrow m$ symmetry of the original model is broken, i.e. at strong disorder we expect an MBL time-crystal with eigenstates close (up to finite-depth local unitary transformation) to the form in Eq. (B3).

Appendix C: Connection between edge chirality and bulk FET order

In this section, we show that the minimal radical CF phase is tied to the bulk FET order in the limit of static \mathbb{Z}_2 gauge fluxes and non-interacting emergent Majorana fermions. In this limit, each gauge-flux sector can be viewed as a free problem where a π -flux binds or unbinds a complex fermion in every Floquet period. This allows us to view the FET order, characterized by the dynamical exchange of m and $e = m \times \psi$ particles, as a gauged version of a Floquet SPT order of the emergent ψ -fermions.

We will first derive expressions for the number of chiral Majorana edge modes, $C \in \mathbb{Z}$, related to the CF edge invariant by:

$$\nu_{\text{CF}} = C \log \sqrt{2}. \quad (\text{C1})$$

Next we will derive an index for the FET order, \mathcal{I}_{FET} , which takes value -1 when the e and m anyons are dynamically exchanged, and is $+1$ otherwise. Finally, we show that the parity of C is equal to \mathcal{I}_{FET} :

$$(-1)^C = \mathcal{I}_{\text{FET}}. \quad (\text{C2})$$

To derive this relation, consider the time evolution on a cylinder with periodic boundary condition in the x direction but open boundary condition in y , and with all dimensions much larger than the Lieb-Robinson length of the Floquet evolution. In the absence of interactions and gauge-flux dynamics, the Majorana operator at position r evolves as:

$$U(T)c_rU^\dagger(T) = \sum_{r'} M_{r,r'} c_{r'} \quad (\text{C3})$$

where M is an orthogonal matrix. Note that $\det(M) = +1$, as required by the topological conservation of fermion parity.

Suppose the Floquet evolution can be made trivial in the bulk by non-chiral finite-depth local unitary transformation (as happens for both the Majorana CF phase and the fermion FSPT phase). Then, after ‘undoing’ the bulk evolution the non-trivial action of $U(T)$ only occurs on a 1D strips near the top and bottom of the cylinders, and M can be written as a direct sum of $M = O \oplus \mathbb{I}_m \oplus O'$. Here, O acts only on a strip with finite extent in y at the top of the cylinder, \mathbb{I}_m is the identity in the middle, and O' acts in a finite y -thickness strip at the bottom of the cylinder.

In the following we will focus on one end of the cylinder, label the Majorana operators by their x position, and an auxiliary flavor label α . Then, we can consider the time-evolution operator restricted to the top of the cylinder: $O_{x,\alpha;x',\beta}$, which is an orthogonal matrix (i.e. can have determinant ± 1 , so long as $\det O = \det O'$).

1. Chiral edge invariant

To gain some intuition, we first study the special case with translation invariance. In this setup we may compute the number of chiral Majorana edge modes via the momentum space winding number (following a straightforward generalization of the results of [15], to Majorana fermions instead of complex ones):

$$C \stackrel{\text{trans. inv.}}{=} \int \frac{dk}{2\pi} \text{tr} \left(\tilde{O}^{-1}(k) i \partial_k \tilde{O}(k) \right) \quad (\text{C4})$$

where $\tilde{O}_{\alpha,\beta}(k) = \int dx e^{ikx} O_{x,\alpha;0,\beta}$, and the tr is over the flavor indices α, β .

Since we are interested in disordered systems, we would like to reformulate this invariant in a way that does not rely on momentum conservation. A useful formal tool is to replace the integral over momenta in Eq. (C4) by an adiabatic flow under the insertion of ‘flux’. Though the fermion charge is not conserved in the present problem with Majorana fermions, we can still formally define a version of O with flux $\theta \in (-\pi, \pi]$ threaded through the bond between $x = 0$ and $x = 1$ along the edge:

$$(O_\theta)_{xx'} = \begin{cases} O_{xx'} e^{i\theta} & \text{for } -\frac{L_x}{2} < x' \leq 0 < x < \frac{L_x}{2} \\ O_{xx'} e^{-i\theta} & \text{for } -\frac{L_x}{2} < x \leq 0 < x' < \frac{L_x}{2} \\ O_{xx'} & \text{otherwise} \end{cases} \quad (\text{C5})$$

where we have suppressed the flavor index, and L_x denotes the circumference of the cylinder edge.

A minor, but formally necessary technical detail is that some truncation scheme is required to make the flux insertion compatible with periodic boundary-conditions. While various equivalent methods are possible, here, we have simply turned off the $e^{i\theta}$ phase twist at a distance $L_x/2$ from the origin. However, the effects of this finite-size truncation can be safely ignored in large systems. Namely, since $|O_{xx'}|$ results from finite time evolution with a local (2D) Hamiltonian, the spatial extent matrix elements are constrained by a Lieb-Robinson bound, i.e. $|O_{x,x'}|$ falls off exponentially as $\sim e^{-|x-x'|/\ell_{\text{LR}}}$ for distances much longer than a Lieb-Robinson length $|x-x'| > \ell_{\text{LR}}$. For similar reasons, O_θ will be exponentially close to a unitary matrix: $\|O_\theta O_\theta^\dagger - \mathbb{I}\| \approx e^{-L_x/\ell_{\text{LR}}}$.

By introducing the adiabatic flow parameterized by θ , the chiral edge invariant can now be written as [24]:

$$C = \int_{-\pi}^{\pi} \frac{d\theta}{2\pi} \text{tr} \left(O_\theta^\dagger i \frac{\partial}{\partial \theta} O_\theta \right), \quad (\text{C6})$$

where the trace runs over all spatial and (the suppressed) flavor indices. One can verify this reproduces Eq. (C4) for translation-invariant edges. If O_θ were exactly unitary, then C would be a winding number which is precisely quantized to integer values. For a large but finite L_x , this integer quantization is accurate up to exponentially

small corrections of order $e^{-L_x/\ell_{LR}}$, due to the truncation at $x = \pm L_x/2$, and becomes exact as $L_x \rightarrow \infty$ limit.

We remark in passing that this invariant can also be formulated directly in the limit of an infinitely long edge, $L_x = \infty$, where the flux-threading can then be implemented by a unitary operator: $O_\theta = e^{i\theta P} O e^{-i\theta P}$, where P is a projection into the subspace with $x > 0$

$$P_{xx'} = \delta_{xx'} \equiv \begin{cases} 1 & \text{for } x > 0 \\ 0 & \text{for } x \leq 0 \end{cases}. \quad (C7)$$

Putting this form of O_θ into Eq. (C6), one finds

$$C = \text{tr} (O^{-1} [P, O]), \quad (C8)$$

In this form, C is the trace of a difference between two projection operators, whose eigenvalues are 0 or 1, and therefore C is precisely quantized to an integer that cannot be altered by smooth deformations (local unitary transformations of O). Related quantities were identified in Refs. [23 and 26] as a ‘flow’ index for causal unitary matrices.

2. FET invariant

To diagnose the FET order, we would like to compare the change in fermion parity with and without a π flux threading the edge. In the FET phase, Floquet evolution toggles the edge between topological and trivial states, and hence pumps an opposite amount of fermion parity dependent on the presence or absence of a π flux. In a non-FET phase, the parity pumped is independent of the flux.

More precisely, such parity pumping is captured by comparing the determinants of O with and without a π flux inserted. To see this, observe that the fermion parity operator for the system $P_F = i^{N_{\text{sites}}} \prod_r c_r$ evolves as:

$$U(T) P_F U(T)^\dagger = (\det O) P_F, \quad (C9)$$

which follows from the antisymmetry of the fermion product and the orthogonality of O . Here, N_{sites} is the number of Majorana sites, and the phase factor is chosen to make $P_F^2 = 1$.

From these considerations, we can readily write the FET invariant as a comparison between O_0 and O_π :

$$\mathcal{I}_{\text{FET}} = \det (O_\pi O_0^{-1}), \quad (C10)$$

which is -1 in the FET phase, and $+1$ otherwise. We note in passing that various equivalent forms for \mathcal{I}_{FET} like $(\det O_\pi / \det O_0)$, or $(\det O_\pi \cdot \det O_0)$, are possible. However, the above formulation is convenient as it remains well defined in the infinite system limit.

3. Relation between C and \mathcal{I}_{FET}

Finally, we relate the chiral edge and bulk FET invariants. First observe that, as O is real,

$$O_\theta = O_{-\theta}^*. \quad (C11)$$

This implies

$$C = \int_{-\pi}^{\pi} \frac{d\theta}{2\pi} \text{tr} (O_\theta^\dagger i \partial_\theta O_\theta) = \int_0^\pi \frac{d\theta}{\pi} \text{tr} (O_\theta^\dagger i \partial_\theta O_\theta), \quad (C12)$$

and therefore

$$\begin{aligned} \mathcal{I}_{\text{FET}} &= \det (O_\pi O_0^{-1}) \\ &= \exp (\text{tr} (\log O_\pi - \log O_0)) \\ &= \exp \left(-i\pi \int_0^\pi \frac{d\theta}{\pi} i \partial_\theta \text{tr} \log O_\theta \right) \\ &= \exp \left(-i\pi \int_0^\pi \frac{d\theta}{\pi} \text{tr} (O_\theta^\dagger i \partial_\theta O_\theta) \right) \\ &= e^{-i\pi C}. \end{aligned} \quad (C13)$$

This establishes the claimed bulk-edge correspondence between the edge chiral unitary invariant and the bulk FET invariant, in the limit of vanishing gauge fluctuations and non-interacting emergent fermions. A more formal proof that also applies to the general interacting case can be obtained using super-algebra methods[28].

Appendix D: Spin- $N/2$ lattice model of chiral parafermion Floquet phase

To obtain solvable models of radical CF phases whose edges implement chiral parafermion translation, we can adapt the driving protocol of Eq. (2), to the \mathbb{Z}_N generalization of Kitaev’s honeycomb model constructed by Barkeshli et al. [35]. We again consider a honeycomb, but with N -state spins rather than 2-state spins on each site. The terms of the driving Hamiltonian are formed out of the unitary single-spin unitary operators $\tau_r^{x,y,z}$, satisfying $(\tau_r^i)^N = 1$, $\tau_r^z = (\tau_r^x \tau_r^y)^\dagger$, and τ ’s on different sites commute: $[\tau_r^i, \tau_{r'}^j] = 0$ ($r \neq r'$), and the operators satisfy the on-site algebra:

$$\tau_r^x \tau_r^y = e^{2\pi i/N} \tau_r^y \tau_r^x \quad (D1)$$

plus identical relations for cyclic permutations of (x, y, z) indices.

Then, simply replacing $S_r^i \rightarrow \tau_r^i$ in Eq. (2) implements the desired irrational chiral Floquet phase. In particular, following [35], we may describe the N -state spins as quartets of parafermionic twist defects with quantum dimension \sqrt{N} (generalizing the Majorana fermion description for $N = 2$), which we can embed spatially around the honeycomb in the $\{c, b^{x,y,z}\}$ positions shown in Fig. 1.

Generalizing the fusion relations for Majorana defects ($N = 2$), these \mathbb{Z}_N twist defects, which we will denote σ , can fuse to any number of the anyonic ψ particles: $\sigma \times \sigma = \sum_{j=0}^{N-1} \psi^j$ and $\psi^j \times \sigma = \sigma$.

As for the spin-1/2 version, it is convenient to pair the bond-centered twist defects, $b^{\ell_{rr'}}$, on bonds $\langle rr' \rangle$ of type $\ell_{rr'} \in \{x, y, z\}$, into \mathbb{Z}_N valued gauge link variables: $\sigma_{rr'} = e^{2\pi i j/N}$, where j is the number of ψ particles in the fusion of the two bond-centered twist defects.

Again, the \mathbb{Z}_N gauge flux through each plaquette:

$$F_P = \prod_{\langle rr' \rangle \cap P} \tau_{rr'}^{\ell_{rr'}} \tau_{r'r}^{\ell_{r'r}} = \prod_{\langle rr' \rangle \cap P} \sigma_{r,r'} \quad (\text{D2})$$

is conserved throughout the Floquet evolution, though this flux operator is now a \mathbb{Z}_N object, having eigenvalues $e^{2\pi i/N}$. Here $\ell_{rr'}$ denotes the type (x, y , or z) of the link $\langle rr' \rangle$.

On flux-free plaquettes ($F_P = 1$), the fusion channel ($\in \{1, \psi, \psi^2, \dots, \psi^{N-1}\}$) of the c parafermions on the left and right corners of the hexagon is also conserved. To make contact with the algebraic anyon language describing a \mathbb{Z}_N gauge theory, we will identify to the configuration where there is a plaquette with zero flux, and parafermions fusing to ψ , as a ψ particle excitation. Sim-

ilarly, we will label plaquettes with parafermions fusing to 1, and a single flux, ($F_P = e^{2\pi i/N}$) as m -excitations, and plaquettes with both parafermions fusing to ψ and $F_P = e^{2\pi i/N}$ as an $e = m \times \psi$ excitation.

Again, the terms $e^{-ih^{[j]}} = \prod_{\langle rr' \rangle \in j} \tau_r^j \tau_{r'}^j$ exchange the site-centered (c) parafermion defects at the ends of j -type bonds. In the bulk, in one Floquet cycle, the two twist defects on the left and right side of a bulk plaquette are braided in a counterclockwise fashion, and hence encircle the \mathbb{Z}_N gauge flux through the plaquette. For plaquettes with n_F fluxes ($F_P = e^{2\pi i j/N}$), braiding of twist defects originally in the fusion channel $\sigma \times \sigma = \psi^k$, around the flux changes the fusion channel of the twist defects by ψ^{j-k} , producing bulk FET order in which e and m particles are interchanged.

At the edge, we again see that the Floquet evolution performs a clockwise chiral translation of one parafermionic twist defect per unit cell. Since the parafermion defects have quantum dimension \sqrt{N} , this produces an irrational chiral Floquet index:

$$\nu = \log \sqrt{N} \quad (\text{D3})$$

-
- [1] Takashi Oka and Hideo Aoki, “Photovoltaic hall effect in graphene,” *Physical Review B* **79**, 081406 (2009).
 - [2] Netanel H Lindner, Gil Refael, and Victor Galitski, “Floquet topological insulator in semiconductor quantum wells,” *Nat. Phys.* **7**, 490–495 (2011).
 - [3] YH Wang, Hadar Steinberg, Pablo Jarillo-Herrero, and Nuh Gedik, “Observation of floquet-bloch states on the surface of a topological insulator,” *Science* **342**, 453–457 (2013).
 - [4] Vedika Khemani, Achilleas Lazarides, Roderich Moessner, and S. L. Sondhi, “Phase structure of driven quantum systems,” *Phys. Rev. Lett.* **116**, 250401 (2016).
 - [5] CW von Keyserlingk and SL Sondhi, “Phase structure of one-dimensional interacting floquet systems. ii. symmetry-broken phases,” *Physical Review B* **93**, 245146 (2016).
 - [6] Dominic V. Else, Bela Bauer, and Chetan Nayak, “Floquet time crystals,” *Phys. Rev. Lett.* **117**, 090402 (2016).
 - [7] CW von Keyserlingk, Vedika Khemani, and SL Sondhi, “Absolute stability and spatiotemporal long-range order in floquet systems,” *Physical Review B* **94**, 085112 (2016).
 - [8] Takuya Kitagawa, Erez Berg, Mark Rudner, and Eugene Demler, “Topological characterization of periodically driven quantum systems,” *Phys. Rev. B* **82**, 235114 (2010).
 - [9] Liang Jiang, Takuya Kitagawa, Jason Alicea, A. R. Akhmerov, David Pekker, Gil Refael, J. Ignacio Cirac, Eugene Demler, Mikhail D. Lukin, and Peter Zoller, “Majorana fermions in equilibrium and in driven cold-atom quantum wires,” *Phys. Rev. Lett.* **106**, 220402 (2011).
 - [10] JK Asbóth, B Tarasinski, and P Delplace, “Chiral symmetry and bulk-boundary correspondence in periodically driven one-dimensional systems,” *Phys. Rev. B* **90**, 125143 (2014).
 - [11] Y. Gannot, “Effects of Disorder on a 1-D Floquet Symmetry Protected Topological Phase,” *arXiv:1512.04190* (2015).
 - [12] Manisha Thakurathi, Aavishkar A Patel, Diptiman Sen, and Amit Dutta, “Floquet generation of majorana end modes and topological invariants,” *Phys. Rev. B* **88**, 155133 (2013).
 - [13] Manisha Thakurathi, K Sengupta, and Diptiman Sen, “Majorana edge modes in the kitaev model,” *Phys. Rev. B* **89**, 235434 (2014).
 - [14] R. Roy and F. Harper, “Periodic Table for Floquet Topological Insulators,” *ArXiv e-prints* (2016), *arXiv:1603.06944 [cond-mat.str-el]*.
 - [15] Mark S Rudner, Netanel H Lindner, Erez Berg, and Michael Levin, “Anomalous edge states and the bulk-edge correspondence for periodically driven two-dimensional systems,” *Phys. Rev. X* **3**, 031005 (2013).
 - [16] Hoi Chun Po, Lukasz Fidkowski, Takahiro Morimoto, Andrew C. Potter, and Ashvin Vishwanath, “Chiral floquet phases of many-body localized bosons,” *Phys. Rev. X* **6**, 041070 (2016).
 - [17] Fenner Harper and Rahul Roy, “Stability of anomalous floquet edge unitaries,” *arXiv preprint arXiv:1609.06303* (2016).
 - [18] Andrew C Potter and Takahiro Morimoto, “Dynamically enriched topological orders in driven two-dimensional systems,” *arXiv preprint arXiv:1610.03485* (2016).
 - [19] Dmitry A Abanin, Wojciech De Roeck, and François

- Huveneers, “Exponentially slow heating in periodically driven many-body systems,” *Phys. Rev. Lett.* **115**, 256803 (2015).
- [20] Dominic V Else, Bela Bauer, and Chetan Nayak, “Prethermal time crystals and floquet topological phases without disorder,” arXiv preprint arXiv:1607.05277 (2016).
- [21] Rahul Nandkishore and David A. Huse, “Many-body localization and thermalization in quantum statistical mechanics,” *Ann. Rev. Cond. Matt. Phys.* **6**, 15–38 (2015).
- [22] Whether stable MBL can occur in dimension higher than one remains an important, unsettled matter of principle[36]. For strong disorder the dynamics will behave as in an MBL system at worst up to super-exponentially long timescale, and possibly forever.
- [23] D Gross, V Nesme, H Vogts, and RF Werner, “Index theory of one dimensional quantum walks and cellular automata,” *Communications in Mathematical Physics* **310**, 419–454 (2012).
- [24] Paraj Titum, Erez Berg, Mark S Rudner, Gil Refael, and Netanel H Lindner, “Anomalous floquet-anderson insulator as a nonadiabatic quantized charge pump,” *Physical Review X* **6**, 021013 (2016).
- [25] Away from this exactly solvable limit, the chiral edge states are protected from localization and necessarily thermalize[16], requiring a redefinition of MBL in terms of dynamics rather than eigenstate order[37, 38].
- [26] Alexei Kitaev, “Anyons in an exactly solved model and beyond,” *Annals of Physics* **321**, 2 – 111 (2006), january Special Issue.
- [27] A Yu Kitaev, “Unpaired majorana fermions in quantum wires,” *Physics-Uspekhi* **44**, 131 (2001).
- [28] L. Fidkowski, Hoi Chun Po, Andrew C Potter, and A. Vishwanath, (to appear).
- [29] Note that, the presence of bulk topological order alone is not enough to elude the rational restriction. Indeed, $U(2T)$ is topologically ordered, but has a rational index.
- [30] Maissam Barkeshli, Chao-Ming Jian, and Xiao-Liang Qi, “Twist defects and projective non-abelian braiding statistics,” *Physical Review B* **87**, 045130 (2013).
- [31] Maissam Barkeshli, Parsa Bonderson, Meng Cheng, and Zhenghan Wang, “Symmetry, defects, and gauging of topological phases,” arXiv preprint arXiv:1410.4540 (2014).
- [32] Andrew C. Potter and Romain Vasseur, “Symmetry constraints on many-body localization,” *Phys. Rev. B* **94**, 224206 (2016).
- [33] Andrew C Potter and Ashvin Vishwanath, “Protection of topological order by symmetry and many-body localization,” arXiv preprint arXiv:1506.00592 (2015).
- [34] Romain Vasseur, Aaron J Friedman, SA Parameswaran, and Andrew C Potter, “Particle-hole symmetry, many-body localization, and topological edge modes,” arXiv preprint arXiv:1510.04282 (2015).
- [35] Maissam Barkeshli, Hong-Chen Jiang, Ronny Thomale, and Xiao-Liang Qi, “Generalized kitaev models and extrinsic non-abelian twist defects,” *Physical review letters* **114**, 026401 (2015).
- [36] Wojciech De Roeck and François Huveneers, “Stability and instability towards delocalization in mbl systems,” arXiv preprint arXiv:1608.01815 (2016).
- [37] A. Chandran, A. Pal, C. R. Laumann, and A. Scardicchio, “Many-body localization beyond eigenstates in all dimensions,” *Phys. Rev. B* **94**, 144203 (2016).
- [38] Rahul Nandkishore and Sarang Gopalakrishnan, “General theory of many body localized systems coupled to baths,” arXiv preprint arXiv:1606.08465 (2016).